THE JOURNAL OF PHYSICAL CHEMISTRY B

Article

pubs.acs.org/JPCB

Role of Formation of Statistical Aggregates in Chlorophyll Fluorescence Concentration Quenching

Wu-Jun Shi,[†] James Barber,[†,‡] and Yang Zhao*[,†]

[†]Division of Materials Science, Nanyang Technological University, Singapore 639798

[‡]Division of Molecular Biosciences, Department of Life Sciences, Imperial College, London SW7 2AZ, United Kingdom

ABSTRACT: Using extensive Monte Carlo simulations, a comprehensive investigation has been carried out on the phenomenon of chlorophyll fluorescence concentration quenching. Our results reveal that statistical aggregations of chlorophylls act mainly as trapping sites for excitation energy and lead to fluorescence quenching. Due to transition dipolar−dipolar interactions between the chlorophylls within a statistical aggregate, the associated oscillator strength changes in comparison to a monomer, and excited energy states show splitting. Further, as the lower energy states are more likely associated with lower oscillator strengths, the fluorescence intensity is observed to decrease. Due to the rapid energy transfer between chlorophyll molecules after photoexcitation, the excitonic energy can easily reach a statistical aggregate, where trapping of the exciton and its subsequent decay occur. With an increase in the chlorophyll concentration, the probability of statistical aggregation increases, thereby accentuating the fluorescence quenching effect.

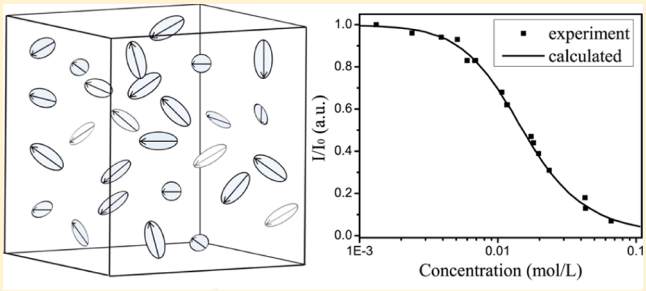

INTRODUCTION

The fluorescence intensity of chlorophyll (Chl) solutions depends peculiarly on the solution concentration. In the limit of low concentration of Chl, the fluorescence intensity is independent of concentration, while at higher concentrations it is found to decrease with an increase in solution concentration. This phenomenon of depletion in fluorescence intensity in concentrated chlorophyll solutions is known as fluorescence concentration quenching, or simply concentration quenching. A number of studies have established its occurrence in different *in vitro* conditions, e.g., by Watson and Livingston in ether solution,[1] by Tweet et al. in monolayers of Chl *a* diluted by long chain alcohols,[2] by Beddard et al. in vesicles and liposomes solution,[3] and by Agrawal et al. in monolayers of dioleoylphosphatidylcholine (DOL) at the nitrogen−water interface.[4] Interestingly, despite the high concentration of Chl in green plants, this phenomenon does not normally occur *in vivo*.

Various studies have subsequently focused on uncovering the underlying mechanism of concentration quenching. Beddard et al. attributed this effect to the transfer of excitation energy to "statistical pairs", i.e., the pairs of Chl's separated by a certain small distance in solutions, which were assumed to act as quenching sites.[5] With a model based on the Förster resonance energy transfer process, they assumed that an excitation arriving at a statistical pair that has an inter-Chl separation equal to or less than a certain threshold would simply be quenched nonradiatively. Effectively, their model contains no mechanism for quenching. Agrawal et al. investigated the fluorescence intensity and lifetime of Chl *a* with real-time measurements in monolayers of Chl *a* and DOL at the nitrogen−water interface.[4] Their results revealed that the fluorescence lifetime of the Chl *a* decreases from 5.5 ± 0.3 to 1.0 ± 0.1 ns when the concentration is increased from 0.0084 mol fraction to 0.080 mol fraction. The fluorescence intensity as well as lifetime was found to exhibit nearly similar profiles as a function of concentration, pointing to the possibility that statistical pairs of Chl *a* may play a role in quenching. Boulu et al. employed a master equation approach to investigate energy transfer and trapping in two-dimensional disordered systems.[6] In their model, the statistical pairs with pigment molecules spaced by less than a critical distance were considered as trapping sites and the Förster transfer rate was employed in considering energy transfer to the traps. By comparing their result with ref 4, the critical separation distance in a statistical pair was found to be 10 Å, while the Förster radius was calculated to be 78 ± 2 Å. However, the more intriguing question of why fluorescence intensity decreases with an increase in solution concentration was largely unanswered until Knox studied the distribution of oscillator strengths associated with close molecular pairs of fixed intermolecular distances.[7] It was argued that, on average, of the two molecular pair states, the lower-lying state corresponds to a smaller oscillator strength. Due to a typically planar conformation, the Chl molecule cannot sustain a completely random orientation when in close vicinity with another. The distribution of oscillator strengths is then

Received: December 1, 2012
Revised: January 30, 2013
Published: March 20, 2013

rendered significantly asymmetric by such a steric constraint, leading to an argument that the statistical pairs exhibit trapping states that are "dark".

Apart from the formation of statistical quenching pairs in solutions, other mechanisms have been proposed in the literature for explaining various fluorescence quenching phenomena. Formation of the excimers has been proposed to explain the concentration quenching of perylene fluorescence in nonpolar solvents such as hydrocarbons in which a second, broad emission appears at longer wavelengths.[8] However, to the best of our knowledge, there is no evidence of excimer formation by Chl *a* in polar solvents, nor are there any concentration-dependent changes in the absorption spectra of the varied systems mentioned earlier.[5,7] Another important mechanism known as collisional quenching or dynamic quenching is often employed to explain fluorescence quenching in solutions, which takes place due to collision between an excited state molecule and a quencher.[9] However, with the use of kinetic modeling to fit fluorescence decay curves, Yuen et al. have proposed the formation of statistical pairs as a more viable mechanism than collisional quenching for Chl *a* in pyridine solutions.[10] As a result, the existing literature on the study of Chl concentration quenching, especially in polar solvents, predominantly considers statistical quenching pair formation as the dominant mechanism. In this work, we thus extend the underlying idea of statistical pair formation by considering the formation of aggregates with multiple Chl *a* molecules.

MODEL AND METHODS

In this work, we have carried out extensive Monte Carlo simulations to study concentration quenching in solutions. The simulation cell consists of a cubic box of length a_0, and 1000 Chl's are distributed randomly in it. Thus, the resulting concentration is proportional to a_0^{-3}. A Chl is modeled as a flat disk of radius equal to 1.0 nm. The smallest separation between two Chl's is set to 0.6 nm. When two Chl's are close enough, a conical region characterized by angle θ_0 is considered as the excluded volume for orientation of the transition dipole to account for steric hindrance, following the approach by Knox.[7] The transition dipole orientation (θ, ϕ) with ϕ (not shown in Figure 1) denoting the azimuthal angle in the *xy* plane is obtained by selecting values from a uniform distribution of random numbers in the ranges specified as $-\cos\theta_0 \leq \cos\theta \leq \cos\theta_0$ and $0 \leq \phi < 2\pi$. Figure 1 shows a corresponding schematic to illustrate the dipolar orientations. In our simulations, we consider the statistical aggregates to act as possible traps for excitation energy. A statistical aggregate is assumed to form if there exists at least one unexcited Chl in the vicinity of an excited Chl within a spherical volume of radius equal to a critical distance (R_{trap}). Thus, as shown in Figure 2, in a 2-aggregate state, there is only one Chl whose distance from an excited Chl is less than R_{trap}, whereas, in a 3-aggregate state, there are two such Chl's, and so on.

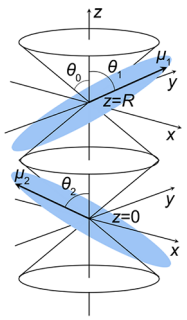

Figure 1. Schematic representation of the orientation of transition dipole moments of two Chl *a*, which lie in planes shown in blue highlights. The conical region in space is the volume excluded for orientation of transition dipoles in a pair of closely spaced Chl *a* molecules.

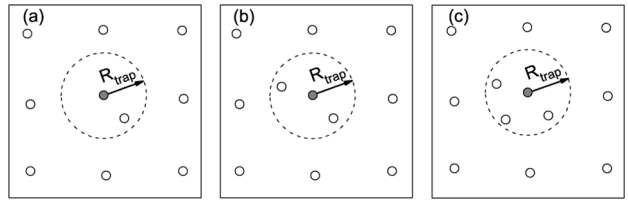

Figure 2. Illustration of statistical aggregates termed as (a) 2-aggregate, (b) 3-aggregate, and (c) 4-aggregate. The filled circles denote an excited Chl, while the ground state Chl's are presented by hollow circles. R_{trap} represents the critical trap radius characterizing the size of aggregates.

We can classify the statistical aggregates into two types based on the comparison of their oscillator strengths (f) with that of a monomer ($f_{monomer}$) and the shift in the energy (ΔE) of excited states due to splitting caused by inter-Chl interactions (see the Appendix).[11−13] The H-type statistical aggregates exhibit $f > f_{monomer}$ ($f < f_{monomer}$) and $\Delta E > 0$ ($\Delta E < 0$), while the J-type statistical aggregates exhibit $f > f_{monomer}$ ($f < f_{monomer}$) and $\Delta E < 0$ ($\Delta E > 0$). In fact, only the lowest excited singlet state can lead to fluorescence emission, because the internal conversion (vibrational relaxation) between the excited levels is so fast ($\sim 10^{-12}$ s) that almost all the excited states will relax to the lowest excited singlet state. For H-type aggregates, the lowest excited state is optically "dark", while, for the J-type, the lowest excited state is "bright". Due to the planar configuration of Chl's, formation of H-type statistical aggregates (i.e., face-to-face geometry) is more likely as compared to J-type statistical aggregates (i.e., end-to-end geometry); however, the dipole−dipole interaction energy in the former configuration is comparatively higher. At a relatively large concentration where the probability of formation of aggregates increases, the dominance of formation of H-type statistic aggregates may be expected to cause a decrease in the fluorescence intensity.

Geometry optimization of the initial structure of Chl *a* obtained as a protein data bank file was carried out with the Gaussian 03 package,[14] by using the density functional theory (DFT) at the B3LYP/6-31G* level.[15,16] On the basis of the optimized geometry, the semiempirical Zerner intermediate neglect of differential orbital method with parameters for spectroscopic properties (ZINDO/S) combined with the configuration interaction singles method (ZINDO/S-CIS), as implemented in the ORCA program,[17] was first employed to calculate the energy difference between the ground state and excited state as well as the oscillator strength of a single Chl *a* molecule. We then consider the two simplest cases of interacting Chl−Chl systems. In the J-aggregate conformation shown in Figure 3a, two Chl's are coplanar with transition dipoles in head-to-tail arrangement. The H-aggregate shown in Figure 3b, on the other hand, has two Chl's in cofacial arrangement with transition dipoles aligned in parallel. We denote the shift in the energies of the lower and higher excited

dx.doi.org/10.1021/jp311821t | J. Phys. Chem. B 2013, 117, 3976−3982

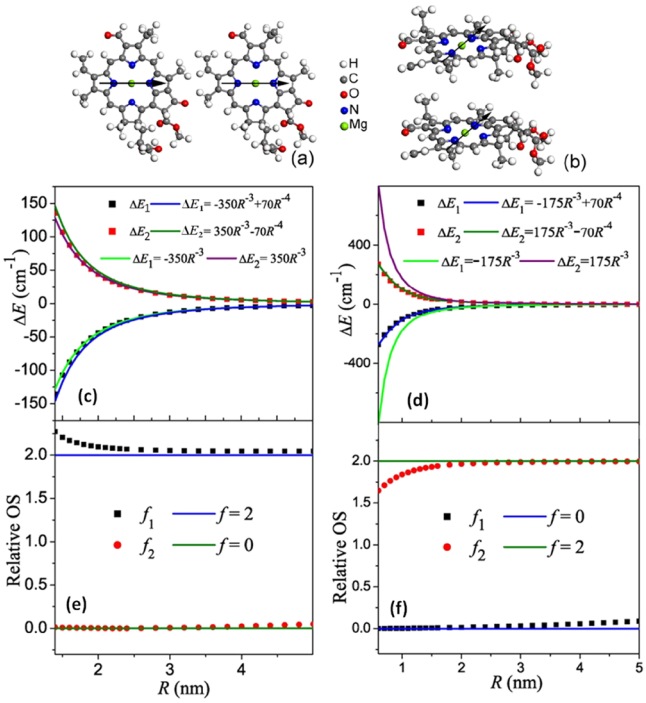

Figure 3. (a) The conformation for two Chl's in head-to-tail arrangement of their transition dipoles (black arrows) or J-aggregate. The associated (c) energy shift of the lower excited state (ΔE_1) and higher excited state (ΔE_2) and (e) relative oscillator strength (OS), i.e., the oscillator strength with respect to that of a monomer, as a function of the distance (R in nm) between central magnesium atoms (green circles), obtained from ZINDO results (filled squares), is plotted together with fitting curves (continuous lines). The right panel corresponds to two Chl's in H-aggregate, i.e., face-to-face conformation.

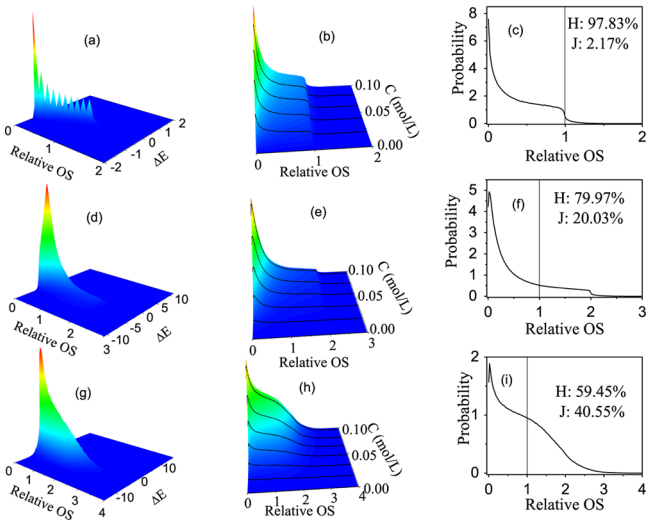

Figure 4. The calculated distribution of transition dipoles for 2-aggregates (a) on oscillator strengths (OS) relative to monomer (OS = 1) and energy shift (ΔE), (b) on relative OS and Chl concentration (C), and (c) as a function of oscillator strength when summed over all values of ΔE. (d–f) Similar plots for 3-aggregates and (g–i) 4-aggregates. The percentage of H-type and J-type in the aggregates is also denoted in the rightmost vertical panel.

states as compared to the excited state energy of a monomer by ΔE_1 and ΔE_2, respectively. We then calculate ΔE_1 and ΔE_2 for both of the conformations of 2-aggregates as a function of the separation between central magnesium atoms. The results obtained for energy shifts corresponding to the J-aggregate are found to be fitted satisfactorily by an R^{-3} dependence curve, as shown in Figure 3c. Note that, due to its geometry, the separation between two Chl's in the J-aggregate must always be greater than the size of a Chl, but for the H-aggregate, it can be comparatively much smaller. Figure 3d shows that, for relatively larger separations (R > 1.4 nm), the energy shift varies with R^{-3} for H-aggregates. The observed R^{-3} dependence of the energy implies that the large distance dipolar–dipolar interaction between Chl's in our simulations is a reasonable approximation. At short distances, however, a correction term with R^{-4} dependence needs to be taken into account. The effect of inclusion of this term is very small for the J-aggregates, as can be observed from Figure 3c. The oscillator strengths corresponding to lower and higher excited state energy levels denoted by f_1 and f_2, respectively, are shown in Figure 3e for the J-aggregate and Figure 3f for the H-aggregate. It can be seen clearly that, for the J-aggregate, the lower excited state is optically bright with its oscillator strength relative to that of a monomer being nearly equal to 2. However, for the H-aggregate, the oscillator strength of the lower excited state is nearly zero, implying it to be an optically dark state. We have calculated further the energies of the charge-transfer states for both the H-type and J-type of aggregates, and found them to be much higher in energy than the first excited state which is a Frenkel exciton state. As a result, such charge-transfer states are less likely to be involved in the low-energy dynamics, which is the focus of this work.

Parts a, d, and g of Figure 4 show the calculated distribution of transition dipoles on oscillator strength relative to monomer and energy shift (ΔE) for 2-aggregates, 3-aggregates, and 4-aggregates, respectively. As described before, we only consider the lowest excited state. It is clear that, for all the cases examined, it is more likely that the lowest lying excited states are associated with lower oscillator strengths. It can be noted that the H aggregates are more likely to exhibit little fluorescence as the probability of nonradiative decay of excitonic energy is large, yet they may still exhibit faint fluorescence depending upon the typically low value of oscillator strength. Similar plots with respect to relative oscillator strength and Chl concentration are shown in Figure 4b, e, and h, wherein it can be easily observed that the probability of formation of the H-type of aggregates grows rapidly with concentration. The most right vertical panel in Figure 4 shows the distribution of transition dipoles when summed over all values of ΔE. While 2-aggregates can be seen to be nearly constituted of just the H-type (>97%), even for 3-aggregates and 4-aggregates, the dominant contribution comes from the H-type at 79.97 and 59.45%.

In this work, we assume the fate of an excited Chl to take up one of the following possible pathways. For a monomer, the excited state can decay via either fluorescence emission or nonradiative process or transfer to other Chl's. Similarly, the excited state of a statistical aggregate can decay via either fluorescence emission or radiationless decay or back transfer to other Chl's (either a monomer or another aggregate). We then define the corresponding rate constants as below:

- K_f is the rate constant for de-excitation of the lowest excited singlet state by fluorescence emission.

dx.doi.org/10.1021/jp311821t | J. Phys. Chem. B 2013, 117, 3976–3982

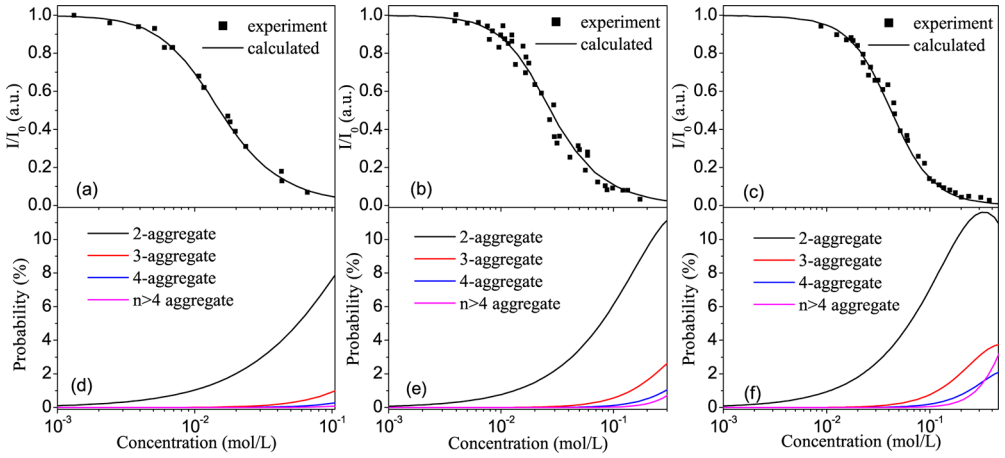

Figure 5. The calculated relative fluorescence intensity (I/I_0) (top panel) and the corresponding probability (bottom panel) of forming 2-, 3-, 4-, and higher-statistical aggregates of Chl *a* as a function of concentration. The experimental data corresponding to Chl *a* in (a) ether is taken from ref 1 and in (b) vesicles and (c) liposomes is taken from ref 3. The Förster radii are 7.0, 6.0, and 4.0 nm in panels a, b, and c, respectively, while the corresponding critical trap radii are 1.1, 1.1, and 1.0 nm.

- K_{none} is the rate constant for de-excitation of the lowest excited singlet state by radiationless decay.
- K_{tran} is the transfer rate constant.

The radiative decay lifetime of large aggregate systems is well-known to differ from that of a monomer.[18] Further, in consideration of the interactions within the statistical aggregates, we need to take into account possible cooperative spontaneous emission of fluorescence, known as superradiance. Earlier studies on light-harvesting complex II (LH-II) in bacterial photosynthetic systems have also established the importance of consideration of superradiance.[19,20] Consequently, the rate constant for the radiative decay process can be written as

$$K_f = \frac{f/f_{monomer}}{\tau_0} \quad (1)$$

where τ_0 is the natural lifetime that can be calculated from the measured molecular absorption spectrum.[21−24] Further, it is typically believed that the nonradiative decay rate for a monomer is smaller than that for aggregates,[25] possibly due to comparatively rapid conformational changes an aggregate may undergo.

The relationship between the fluorescence yield (φ) and the fluorescence lifetime (τ) is typically expressed as

$$\tau = \varphi\tau_0 \quad (2)$$

As a monomer or an aggregate can undergo fluorescence or nonradiative decay of excitation, the fluorescence lifetime that is measured in experiments can be written as[23]

$$\frac{1}{\tau} = \frac{1}{\tau_0} + \frac{1}{\tau_{none}} \quad (3)$$

where $\tau_{none}^{-1} = K_{none}$ corresponds to the rate of nonradiative decay.

Using the data in low concentration regimes at which $\tau = 5.1$ ns and $\varphi = 0.33$,[21] we can estimate τ_0 for a monomer from eq 2 and subsequently $K_{none}^{monomer} = 1/7.5$ ns^{-1} from eq 3. Further, we first assume that the high concentration regime is dominated by statistical pairs or 2-aggregates. The natural lifetime for 2-aggregates can be calculated from their oscillator strengths from eq 1. The fluorescence lifetime for a 2-aggregate is a function of separation between the Chl's (R), and we assume that $\tau = CR$ with C a constant. Further, with the majority of aggregates formed at high concentration regime being likely dimers, we assume that the total decay rate for any aggregate is the same as that for a 2-aggregate.

In our calculations, we employ the Förster type resonance energy transfer mechanism for excitation energy transport between Chl's spaced by a relatively large distance. The transfer rate is then proportional to R^{-6}, where R is the separation between an excited and an unexcited Chl. It was demonstrated by Wong et al. that, in the regime of very small inter-Chl separation, the Förster transfer rate may not be accurate.[22] We thus employ the Coulomb resonance transfer rate for such cases, wherein the transfer rate is proportional to R^{-2}.

The transfer rate from an excited Chl to the ith unexcited Chl is then given as

$$K_{tran}^{i} = \begin{cases} \frac{1}{\tau_C}\left(\frac{R_C}{R_i}\right)^2 & R_i < R_C \\ \frac{1}{\tau}\left(\frac{R_F}{R_i}\right)^6 & R_C \le R_i \le R_F \\ 0 & R_i > R_F \end{cases} \quad (4)$$

where R_i is the separation between the two Chl's and R_F is the Förster transfer radius at which the transfer rate is equal to the monomer fluorescence emission rate τ^{-1}.[22] τ_C is the critical lifetime when the separation between the excited Chl and the ith unexcited Chl is R_C, which in turn is the critical Coulomb resonance transfer distance that can be calculated simply as

$$R_C = R_F\left(\frac{\tau_C}{\tau}\right)^{1/6} \quad (5)$$

The total transfer rate constant is

$$K_{tran} = \sum_{i}^{N} K_{tran}^{i} \quad (6)$$

Therefore, the probability for an exciton to transfer to the ith unexcited Chl is

dx.doi.org/10.1021/jp311821t | J. Phys. Chem. B 2013, 117, 3976−3982

$$P_i = \frac{K_{tran}^{i}}{K_{tran}} \quad (7)$$

In simulating the exciton dynamics, we employ the Markov process of 50 000 random sample cases. We first introduce an exciton by randomly selecting a Chl. We then calculate the rate constants of all the possible processes available to the excited Chl. The evolution of excitonic energy transfer along one of the possible ways is then determined in a probabilistic manner. The exciton may undergo fluorescence or transfer to a new Chl within a sphere of radius R_F around the excited Chl or undergo radiationless decay. If the exciton is not decayed by fluorescence or radiationless quenching, then it is transferred to a new neighboring Chl, and this process is continued until the excitonic energy is ultimately expended. We have also verified that the probability of excitation reaching the edge of the box, when it initially resides near the box center, is negligibly low, thereby eliminating any adverse effects of finite sized simulation cell. The methodology adopted here follows similar reasoning to that used by Imbusch et al. in his study of excitation energy transfer in ionic systems such as ruby.[24]

RESULTS AND DISCUSSION

The results of fitting the experimental data corresponding to Chl *a* fluorescence measurements in different media with the calculated relative fluorescence intensity are shown in Figure 5, and a satisfactory comparison can be easily observed. In all our calculations, τ = 5.1 ns which is the lifetime observed at infinite dilution experimentally,[3,21] while τ_C = 5.1 ps is set to be 3 orders of magnitude smaller than τ to account for much higher transfer rate at a close distance, and C = 0.1 ns/nm. The critical distance corresponding to Coulomb resonance energy transfer is calculated by eq 5. In panel a, the Förster transfer distance was taken as R_F = 7.0 nm, while the radial expanse of statistical aggregates was taken as R_{trap} = 1.1 nm. The values of these two parameters in panel b are R_F = 5.0 nm and R_{trap} = 1.1 nm, while, in panel c, they are taken as R_F = 4.0 nm and R_{trap} = 1.0 nm.

The lower panel in Figure 5 shows the probability of formation of different types of aggregates with increasing concentration for a specified R_{trap}. The values of R_{trap} are identical in panels d and a, in panels e and b, and in panels f and c. It can be observed that there are negligibly small fractions of statistical aggregates formed at low concentration, since the average separation between Chl's is relatively large. However, at the high concentration regimes, different types of statistical aggregates start to appear. The emergence of statistical aggregates is interlinked to the concentration quenching, since aggregates can act mainly as the trapping sites for the excitation energy. This process primarily competes with the fluorescence emission. Due to the dipole−dipole interactions between Chl's in a statistical aggregate, its oscillator strength is more likely to diminish compared to that of the monomer (eq A9), thereby causing the fluorescence intensity to change. At high enough concentrations, rapid transport of excitonic energy among the Chl's allows the exciton to reach an aggregate before fluorescence takes place. Excitonic trapping in statistical aggregates, which are predominantly of H-type, increases the probability of fast nonradiative relaxation significantly, thereby quenching the fluorescence. It is notable here that earlier experimental results indicate a negligible back transfer from an excited dimer to a monomer.[25] However, unlike earlier studies which considered statistical pairs as absolute traps of excitation energy,[5,6,25] in this work, we have incorporated the possibility of such back transfer from an aggregate, allowing us to delve into a possibly more accurate physical picture. We also note that, if the chemical traps are open such as *in vivo*, then the transfer to a chemical trap would have to compete with trapping by statistical aggregates.[5]

In our simulations, we have chosen different values of Förster radius while fitting data for different solvents, which can be justified to originate from differences in refractive indices of the solvents. The critical trap radius, on the other hand, is associated with the tendency of aggregation of Chl molecules. Presuming that the influence of interaction between solvent molecules and Chl *a* molecules on the intermolecular interactions between Chl *a* is only marginal, the critical trap radius may accordingly vary only a little. Beddard et al. had found more prominent fluorescence quenching in Chl *a* in vesicle solutions as compared to that in liposome solutions and attributed it to the curvature effects resulting from structural differences between vesicles and liposomes.[3] Results obtained in this work with respect to fitting to experimental data of Beddard et al. indicate that the difference in R_F is more important. The Chl distribution in vesicles and liposomes may be subjected to certain spatial restrictions owing to their structured assembly with Chl's. However, excellent fitting obtained in the current work suggests that our model based on a completely random distribution of Chl's may work reasonably well even for these cases. We thus propose that such differences in quenching concentrations arise likely from the difference in the index of refraction which can affect the Förster radius significantly. We speculate that a possible corroboration of our arguments may be obtained through future experiments in which the full width of half-maximum and the Stokes shift are measured and compared for different solvents.

CONCLUSION

In summary, we have investigated the phenomenon of fluorescence concentration quenching via Monte Carlo simulations of a model system of randomly distributed Chl *a* molecules. We have employed distance dependent excitation energy transfer mechanisms, *viz.*, short ranged Columbic resonance transfer and long ranged Förster type resonant energy transfer, to study the transport of excitonic energy between the Chl's. We account for the aggregation effects in concentrated solutions by modeling the formation of statistical aggregates of certain specified size. It is argued that such aggregates may act mainly as trapping sites for an inbound exciton and eventually cause its quenching via radiationless decay as the excited states associated with the preferentially formed H-type aggregates are optically dark. The rapid transfer between Chl's allows excitonic energy to reach an aggregate on a time scale shorter than that for its fluorescent decay. The pronounced fluorescence quenching at high concentrations is found accordingly to originate from the enhanced probability of formation of statistical aggregates, of H-type in particular. Satisfactory agreement with various experimental results has also been achieved, lending support to the proposed mechanisms of concentration quenching. This work is thus hoped to illuminate intriguing aspects of the fluorescence quenching process in chlorophyll molecules in concentrated solutions.

dx.doi.org/10.1021/jp311821t | J. Phys. Chem. B 2013, 117, 3976−3982

APPENDIX: CALCULATION OF OSCILLATOR STRENGTH AND ENERGY SHIFTS

The theory of the spectral properties of aggregates of dye molecules has earlier been proposed for dimers and trimers.[26] Here, we extend this theory for a general scenario of aggregates formed with N molecules or N-aggregates.

The Hamiltonian for such a system can be written as

$$H = \sum_i H_i + \sum_{i>j} V_{ij} \tag{A1}$$

where H_i is the Hamiltonian of the ith isolated Chl and V_{ij} corresponds to the interaction energy between the ith and jth Chl's. Let $|\Phi_{1g}\rangle$, $|\Phi_{2g}\rangle$, $|\Phi_{3g}\rangle$, ..., $|\Phi_{Ng}\rangle$ ($|\Phi_{1e}\rangle$, $|\Phi_{2e}\rangle$, $|\Phi_{3e}\rangle$, ..., $|\Phi_{Ne}\rangle$) represent the electronic ground (excited) states of the monomers. The ground state wave functions for the ith statistical aggregate then become

$$|\Psi_{ig}\rangle = \prod_j |\Phi_{jg}\rangle \tag{A2}$$

while the corresponding excited state wave functions can be written as

$$|\Psi_{ie}\rangle = |\Phi_{ie}\rangle \prod_{j\neq i} |\Phi_{jg}\rangle \tag{A3}$$

To calculate the electronic states of the aggregates, the Schrödinger equation can be solved using the above Hamiltonian (eq A1). We then assume V_{ij} to be sufficiently weak to allow us to approximate the ground-state wave function to stay the same as $|\Psi_{ig}\rangle$, while the excited-state wave functions are given by $|\Psi_{ie}\rangle$. The complete wave function as a linear combination of all the excited states can be calculated from

$$|\Psi_i\rangle = \sum_j C_j |\Psi_{je}\rangle \tag{A4}$$

where C_j are the eigenvector coefficients that can be solved from the Schrödinger equation:

$$\begin{pmatrix} E_1 & V_{12} & \dots & V_{1N} \\ V_{21} & E_2 & \dots & V_{2N} \\ \vdots & \vdots & \ddots & \vdots \\ V_{N1} & V_{N2} & \dots & E_N \end{pmatrix} \begin{pmatrix} C_1 \\ C_2 \\ \vdots \\ C_N \end{pmatrix} = E \begin{pmatrix} C_1 \\ C_2 \\ \vdots \\ C_N \end{pmatrix} \tag{A5}$$

where E_1, E_2, ..., E_N denotes the on site energy:

$$E_i = \langle \Psi_{ie}|H|\Psi_{ie}\rangle - \langle \Psi_{ig}|H|\Psi_{ig}\rangle \tag{A6}$$

and V_{ij} is the interaction between the ith and jth Chl's

$$V_{ij} = \langle \Psi_{ie}|H|\Psi_{je}\rangle \tag{A7}$$

Solving the Schrödinger equation yields N energy eigenvalues (E_i) and corresponding eigenvectors (C_1, C_2, ..., C_N).

We consider the interaction between Chl's as the dipole–dipole interaction[11]

$$V_{ij} = \frac{\mu_i \mu_j}{4\pi\epsilon R_{ij}^3}[\hat{\mu}_i \cdot \hat{\mu}_j - 3(\hat{\mu}_i \cdot \hat{r})(\hat{\mu}_j \cdot \hat{r})] \tag{A8}$$

where μ_i (μ_j) are the transition dipole moments of the ith (jth) Chl's with their directions along the unit vectors $\hat{\mu}_i$ ($\hat{\mu}_j$), ϵ is the dielectric constant of the medium, R_{ij} is the distance between the two Chl's, and $\hat{r}$ is the corresponding unit vector.

Finally, the oscillator strength of the aggregates (f_i) corresponding to the ith excited energy state (E_i) is calculated as

$$f_i = f_{\text{monomer}} |\sum_j C_{ij}\hat{\mu}_j|^2 \tag{A9}$$

where f_{monomer} is the oscillator strength of a monomer. The difference between the ith eigenvalue and ith on site energy, here called the energy shift ΔE, is given as

$$\Delta E = E - E_i \tag{A10}$$

AUTHOR INFORMATION

Corresponding Author

*E-mail: yzhao@ntu.edu.sg.

Notes

The authors declare no competing financial interest.

ACKNOWLEDGMENTS

We dedicate this paper in memory of Lord George Porter, Nobel Laureate who died 10 years ago and who was the first to identify concentration quenching of chlorophyll fluorescence as a unique phenomenon. Support from the Singapore National Research Foundation through the Competitive Research Programme (CRP) under Project No. NRF-CRP5-2009-04 is gratefully acknowledged. The authors thank Prathamesh Mahesh Shenai, Liwei Duan, and Lipeng Chen for many helpful discussions.

REFERENCES

(1) Watson, W. F.; Livingston, R. *J. Chem. Phys.* **1950**, *18*, 802–809.
(2) Tweet, A. G.; Bellamy, W. D.; Gaines, G. L. *J. Chem. Phys.* **1964**, *41*, 2068–2077.
(3) Beddard, G. S.; Carlin, S. E.; Porter, G. *Chem. Phys. Lett.* **1976**, *43*, 27.
(4) Agrawal, M. L.; Chauvet, J. -P; Patterson, L. K. *J. Phys. Chem.* **1985**, *89*, 2979–2983.
(5) Beddard, G. S.; Porter, G. *Nature* **1976**, *260*, 366–367.
(6) Boulu, L. G.; Patterson, L. K.; Chauvet, J. P.; Kozak, J. J. *J. Chem. Phys.* **1987**, *86*, 503–507.
(7) Knox, R. S. *J. Phys. Chem.* **1994**, *98*, 7270–7273.
(8) Ferreira, J. A.; Porter, G. *J. Chem. Soc., Faraday Trans.* **1977**, *2* (73), 340.
(9) Valeur, B. *Molecular Fluorescence. Principles and Applications*; Wiley-VCH: Weinheim, Germany, 2002.
(10) Yuen, M. J.; Shipmanj, L. L.; Katz, J.; Hindman, J. C. *Photochem. Photobiol.* **1980**, *32*, 281–196.
(11) Kasha, M.; Rawis, H. R.; El-Bayoumi, M. A. *Pure Appl. Chem.* **1965**, *11*, 371–392.
(12) del Monte, F.; Ferrer, M. L.; Levy, D. *Langmuir* **2001**, *17*, 4812–4817.
(13) McRae, E. G.; Kasha, M. *J. Chem. Phys.* **1958**, *28*, 721–722.
(14) Frisch, M. J.; Trucks, G. W.; Schlegel, H. B.; Scuseria, G. E.; Robb, M. A.; Cheeseman, J. R.; Montgomery, J. A., Jr.; Vreven, T.; Kudin, K. N.; Burant, J. C.; et al. *Gaussian 03*, revision D.01; Gaussian, Inc.: Wallingford, CT, 2004.
(15) Hehre, W. J.; Ditchfield, R.; Pople, J. A. *J. Chem. Phys.* **1972**, *56*, 2257–2261.
(16) Becke, A. D. *J. Chem. Phys.* **1993**, *98*, 5648–5652.
(17) Neese, F. *An ab initio, DFT and semiempirical electronic structure package, ORCA*, version 2.8; University of Bonn: Bonn, Germany, 2010.
(18) Rehler, N. E.; Eberly, J. H. *Phys. Rev. A* **1970**, *3*, 1735–1751.
(19) Meier, T.; Zhao, Y.; Chernyak, V.; Mukamel, S. *J. Chem. Phys.* **1997**, *107*, 3876–3893.

(20) Zhao, Y.; Meier, T.; Zhang, W. M.; Chernyak, V.; Mukamel, S. *J. Phys. Chem. B* **1999**, *103*, 3954−3962.
(21) Brody, S. S. *Photosynth. Res.* **2002**, *73*, 127−132.
(22) Wong, K. F.; Bagchi, B.; Rossky, P. J. *J. Phys. Chem. A* **2004**, *108*, 5752−5763.
(23) Govindjee; Mar, T.; Singhal, G. S.; Merkelo, H. *Biophys. J.* **1972**, *12*, 797−808.
(24) Imbusch, G. F. *Phys. Rev.* **1967**, *153*, 326−337.
(25) Lutz, D. R.; Nelson, K. A.; Gochanour, C. R.; Fayer, M. D. *Chem. Phys.* **1981**, *58*, 325−334.
(26) Cenens, J.; Schoonheydt, R. A. *Clays Clay Miner.* **1988**, *36*, 214−224.